

Development of mathematical and computer models of fiber-optic sensors, based on periodic Bragg structures

Aliya Kalizhanova^{1,3}, Murat Kunelbayev^{1,2*}, Ainur Kozbakova^{1,3}, Zhalau Aitkulov⁴, Zhassulan Orazbekov⁵

^{1,2}Al - Farabi Kazakh National University, Kazakhstan, Institute of Information and Computational Technologies CS MES RK, Kazakhstan

³Almaty University of Power Engineering and Telecommunications, Kazakhstan,

⁴Academy of Logistics and Transport, Kazakhstan

⁵Abai Kazakh National Pedagogical University, Kazakhstan

Received: March 21, 2021. Revised: February 3, 2022. Accepted: March 15, 2022.

Published: April 5, 2022.

Abstract- In the article there have been considered the issues of mathematical and computer modeling of fiber Bragg grating's, using the method of transfer matrix. Method of transfer matrix allows specify the spectral characteristics of optical components, based on theory of bound modes and matrix description of electromagnetic wave, passing through optic fiber. There have been analyzed fiber Bragg grating's with different lengths in accordance with spectral characteristics, such as, transmittance and reflection spectra. As well, there was carried out the experiment with influence of various parameters at fiber Bragg grating's spectral characteristics. Fiber Bragg grating's spectral characteristics were studied and optimal grating parameters were selected for developing the fiber-optic sensors, based on fiber Bragg grating's. Developed and studied a computer model of flow-diagram of communication modes theory and Transfer Matrix Method. From the studied model it might be noticed, that in MATLAB software, selected for modeling, were formed for implementation into the MATLAB code. As well, in MATLAB software there were used fiber Bragg grating's principal features and selected for studying influence of external factors, such as deformation, strain and temperature at FBG sensor's reflection spectrum.

Key words: fiber Bragg grating, fiber-optic sensors, temperature, mathematical modeling, apodization.

I. INTRODUCTION

At present there is a lot of technical devices, failure of which can lead not only to huge financial losses, but, also, to threat to environment. Therefore, an important problem is effective diagnostics of health, including electronic components and check of their operating conditions. Early detection of mistake permits to introduce preventive measures and avoid serious consequences. Measuring systems, based on optoelectronic systems are used in machines and processes diagnostics [1]. Of

special role are optic fiber sensors, which have a number of advantages, among them the most important are immunity to electromagnetic interference, low mass and possibility to embedding them into being measured structure [2]. In case of sensor systems, based on fiber Bragg gratings, important advantages are independence of measurement accuracy on light source fluctuation and possibility to create advanced measuring systems, locating several sensors on one optical fiber. Fiber Bragg gratings in sensitive applications are of persistent interest for the scientists all over the world within many years. Their main property is ability to reflect optical radiation with well-defined wave length, with simultaneous transparency for the light with different wave lengths [3], [4].

Based on determining the offset of relative central wave length, fluctuation of light source optical capacity does not affect its accuracy. There exists a lot of techniques for defining Bragg wavelength, which also permits to specify it on the base of spectra, containing great noise [5], [6]. Linear processing of the measured values upon transmitting the shift of significant wave length, called the central length of Bragg wave, makes them natural transformers of physical magnitudes, such as, force [7-9], temperature or deformation [10], [11].

Parameter, exercising definite influence upon the form of Bragg grating spectrum, is apodization. In the simplest case, authors differentiate uniform gratings, in which the depth of modulation of interference fringes disturb ratio is equal along the total length of structure. Multitude of definite usage of fiber-optic uniform structures made to introduce apodized functions into their fabrication methods, which brought to variable depth of modulation of grating fringes' refraction index.

One of most frequently used method for temperature sensor interrogation on the base of fiber Bragg gratings is filtering by means of the second grating with the same central wave length, created in similar initial conditions [12]. In such system an important parameter, conditioning effectiveness of the given periodic structure, is minimization of the so-called side lobes [13]. One means of achieving that effect is apodization, changing

modulation depth of refraction index in the core of optical fiber along its axis. Fabrication of periodic structures with any functions of apodization is often linked with the necessity to restructure the system and, therefore, the possibility to use mathematical models to model the spectrum of a grating with the denoted apodization is feasible.

The difference between the current study and the available literature lies in the fact that a new mathematical and computer model of the fiber Bragg connection, made in the MatLab program, has been developed, and a new design has been developed and investigated for the manufacture of periodic structures in optical fibers using the phase mask method. This study is useful for the readers of your esteemed journal, because this topic is relevant all over the world and has more respectful data than other studies.

II. MANUFACTURING TILTED GRATING FBG SENSORS

In 2020 the Institute of information and computational technologies, Ministry of education and science, Republic of Kazakhstan, developed and researched the fiber-optic refractometer

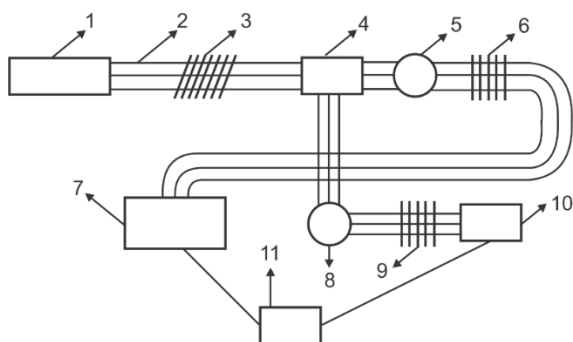


Figure 1. Principal diagram of fiber-optic refractometer (sensor)

Fig.1 shows Principal diagram of fiber-optic refractometer. Operation of the installation being offered is fulfilled as follows.

Fiber-optic refractometer consists of wideband light source 1, connected via multimode optical fiber 2 to Bragg tilted grating 3, which is linked by means of multimode optical connector 4 with two optical circulators 5 and 8. The first outlet of optical connector 4 is coupled by means of multimode optical fiber 2 with the first optical circulator 5, to which it is switched on with the help of multimode optical fiber 2, where the first Bragg grating 6 with linear variable period is connected through the first optical circulator 5 to multimode optical fiber 2 with the first photo detector 7. In distinction to that, the second outlet of optical connector 4 is doubled through multimode optical fiber 2 with the second optical circulator 8, which is, by means of multimode fiber 2 connected to the second Bragg grating with linear variable period 9, which is additionally linked via the second optical circulator 8 by means of multimode optical fiber 2 with the second photo detector 10. Two photo detectors are connected to microcontroller 11.

Novelty of the given fiber-optic refractometer is the fact, that the given fiber-optic refractometer, connected to Bragg tilted grating is considerable simplification of environment refraction index measuring system, as well, it does not demand using of spectrophotometers and optical spectrum analyzers and algorithms for optical spectrum analysis. Invention's important feature is measurements independence on ambient temperature and electromagnetic field influence at measuring point, which is achieved by the fact, that gratings are recorded on one and the same multi-mode fiber. Application of fiber-optic refractometer also eliminated the problem of light sources power fluctuations, as the reflective index measure is the ratio of power, measured with two photo detectors.

Figure 2 shows a fiber-optic sensor for monitoring the condition of engineering and building structures. As well, distinction is the fact, that fiber-optic refractometer consists of a wideband light source with a wide beam, connected via multimode optical fiber to Bragg tilted grating, which is doubled by means of multimode optical fiber with optical connector, and outlet of the first optical connector is linked, by means of multimode optical fiber with the first optical circulator, with which the first Bragg grating with linear variable period is connected with the help of multimode optical fiber, which is additionally linked through the first optical circulator via multimode optical fiber with the first photo detector, whereas the optical connector second outlet is switched on for multimode optical fiber to the second optical circulator, which by means of multimode optical fiber is connected to the second Bragg grating with linear variable period, which is additionally switched on through the second optical circulator, it uses one photo detector (1,5 hours), to the second photo detector.

In fiber-optic refractometer the light source might have high coherence and might be fabricated in the form of fiber or helium-neon laser.

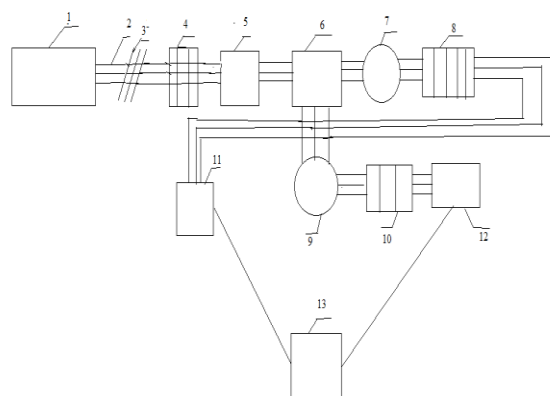


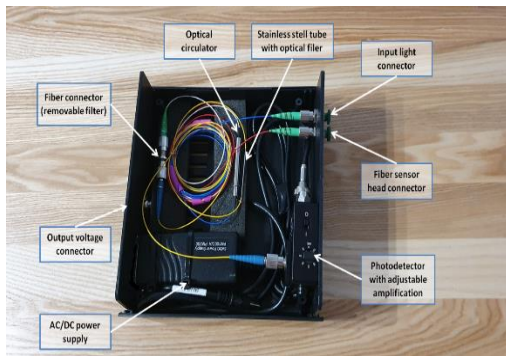
Figure 2. Fiber-optic sensor for monitoring the condition of engineering and building structures

Figure 2 shows a fiber-optic sensor for monitoring the condition of engineering and building structures. The fiber-optic sensor consists of a broadband light source 1 connected via a multimode optical fiber 2 with an inclined Bragg grating 3, which is connected to a special metal diaphragm 4, which deflects the cantilever 5 by deforming. When the cantilever is deflected, the sensitivity to temperature, pressure and bending increases. By means of a multimode optical connector 6

with two optical circulators 7 and 9. The first output of the optical connector 6 is connected using a multimode optical fiber 2 to the first optical circulator 7, to which it is connected using a multimode optical fiber 2, where the first Bragg grating 8 with a linearly variable period is connected through the first optical circulator 7 with a multimode optical fiber 2 to the first photodetector 11. In contrast, the second output of the optical connector 6 is connected via a multi-fiber optical fiber 2 to a second optical circulator 9, which is connected via a multimode fiber 2 to a second Bragg grid with a linearly variable period 10, which is additionally connected via a second optical circulator 9 using a multimode optical fiber 2 to a second photodetector 12. Two photodetectors 11 and 12 are connected to a microcontroller 13.



a)



b)

Figure 3. Fiber-optic sensor for monitoring engineering and building structures health a) mockup; b) sensor interiority

Figure 3 shows a fiber-optic sensor for monitoring the condition of engineering and building structures. Developed fiber-optic sensor to monitor engineering and building structures health consists of:

• Power supply unit of alternate / direct current with 230-240V coupler

- Inlet light coupler
- Connector of fiber sensor head
- Optical circulator
- Optical filter, adjusted to sensor properties, coated with stainless steel tube
- Fiber connectors, maintaining filter removal

- Photo detector with controlled gain
- Output pressure coupler

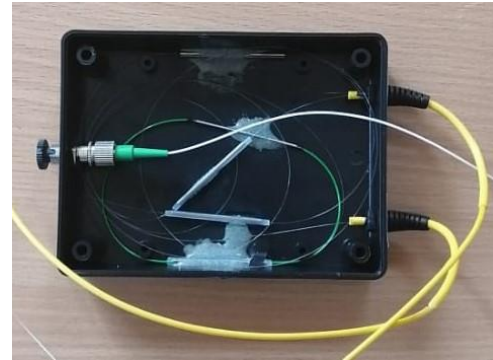


Figure 4. Conventional Bragg fiber-optic sensor

III. MATHEMATICAL MODEL OF APPROXIMATED BRAGG GRATINGS

One of modeling techniques is transfer matrix method (TMM), [14], which permits to define spectral characteristics of optical elements on the base of bounded modes and matrix description of electromagnetic wave, passing through subsequent periods of optical fiber [15]. In that approach we assume, that total length of L grating is divided into exactly definite number of sections N , so that each section, formed as a result with the length $\Delta z = L/N$, might be considered as uniform. Transfer matrix, describing the i - section, will be specified [16]:

$$T_i = \begin{bmatrix} \cosh(\gamma\Delta z) - \frac{\sigma}{\gamma} \sinh(\gamma\Delta z) & -i \frac{k}{\gamma} \sin(\gamma\Delta z) \\ i \frac{k}{\gamma} \sin(\gamma\Delta z) & \cosh(\gamma\Delta z) - \frac{\sigma}{\gamma} \sinh(\gamma\Delta z) \end{bmatrix} \quad (1)$$

For the denoted above definition it is, as well, supposed, that κ - variable component of coupling index for refraction factor contrast ratio $v=1$, analyzed wave length λ and assumed apodized function $g(z)$:

$$k = \frac{\Pi}{\lambda} \cdot v \cdot \hat{\sigma}_{eff}(z) \quad (2)$$

$$\bar{\delta}_{eff}(z) = \delta_{eff} \cdot g(z) \quad (3)$$

During modeling Bragg grating the value of variable coupling index component κ depends on selecting the envelope function of refraction index (2). Complete coupling index is defined by equation (4). It is, as well, known, that λ_B – Bragg wave length, and n_{eff} - effective refraction index.

$$\hat{\sigma} = \delta + \sigma - \frac{1}{2} \frac{d\phi}{dz} \quad (4)$$

$$\delta = 2\pi n_{eff} \left(\frac{1}{\lambda} \cdot \frac{1}{\lambda_B} \right) \quad (5)$$

$$\sigma = \frac{2k}{\nu} \quad (6)$$

Parameter γ for transfer matrix is specified as follows:

$$\gamma = \sqrt{k^2 + \delta^2} \quad (7)$$

Characteristics of total grating might be described as

$$\begin{bmatrix} R_0 \\ S_0 \end{bmatrix} = T \begin{bmatrix} R_N \\ S_N \end{bmatrix} \quad (8)$$

$$T = [T_N] \cdot [T_{N-1}] \cdot \dots \cdot [T_3] \cdot [T_2] \cdot [T_1] \quad (9)$$

Values of matrix parameters T can be used for defining the characteristics both of reflected (10) and transmitted (11) waves. Afterwards, indexed elements T_{ij} denote values of components under i- column and j- transfer matrix row.

$$R = \frac{T_{21}}{T_{11}} \quad (10)$$

$$S = \frac{1}{T_{11}} \quad (11)$$

Transfer Matrix Method is used to define reflection factor of uniform Bragg grating at even or uneven deformation. In the method there was used different FBG features, gap gage has been broken down into N sections of smaller size, with uniform cohesiveness, N amount of sections cannot be arbitrarily large, as large cohesion demands several periods of grating, consequently, N is restricted as:

$$N \leq \frac{2\pi n_{eff} L}{b} \quad (12)$$

In the equation (1) z –length of each section, and in the equation (7) T-matrix for the whole grating can be recorded as:

$$\begin{bmatrix} R(-\frac{L}{2}) \\ S(-\frac{L}{2}) \end{bmatrix} = T \begin{bmatrix} R(\frac{L}{2}) \\ S(\frac{L}{2}) \end{bmatrix} \quad (13)$$

Reflective capacity of Bragg grating designed as wave length function as follows:

$$r(\lambda) = \left[\frac{S(-\frac{L}{2})}{R(-\frac{L}{2})} \right]^2 \quad (14)$$

One of principal parameters in the sensors is Bragg wave length. It has periodic change of refraction index and it is of interest for defining the reflecting length of structure's wave, which is called effective refraction factor (it is

average refraction index). Length of grating and its strength are other parameters. As well, stress, strain, temperature are FBG's external parameters. Parameters, used for modeling FBG sensor, are discussed in succeeding subsections.

A. Stress

Applied axial deformation will shift along Bragg wavelength λ_{BLS} [18]:

$$\lambda_{BLS} = \lambda_B (1 - P_e) \varepsilon_z \quad (15)$$

where λ_B – Bragg wave length, z – applied deformation along longitudinal axis, and P_e - effective tensometric coefficient. P_e depends on several parameters, as it is shown in the following equation

$$P_e = \frac{n_{eff}^2 [P_{12} - \nu(P_{11} + P_{12})]}{2} \quad (16)$$

where P_{11} and P_{12} are Pockells constants, also known as g, components of tensor of fiber-optic deformations, which can be defined experimentally, n_{eff}^2 – effective refraction index, and ν - Poisson's ratio [18].

B. Temperature

Proceeding from ΔT temperature change Bragg wave length shift λ_{BLT} is assigned with following equation [19]:

$$\lambda_{BLT} = \lambda_B (\alpha + \zeta) \delta_T \quad (17)$$

$$\alpha = \frac{\partial(\Lambda) / \partial(T)}{\Lambda} \quad (18)$$

$$\zeta = \frac{\partial(n_{eff}) / \partial(T)}{n_{eff}} \quad (19)$$

where δT – temperature change, λ – grating period, α – fiber heat-expansion coefficient and ζ – thermal-optical coefficient.

C. Strain

Bragg wavelength deformation λ , as a result of ΔP strain change is described with an equation [19]:

$$\Delta \lambda_p = \lambda_B \left[-\frac{(1-2\nu)}{E} + \frac{n_{eff}^2 (1-2\nu)(2P_{12} + P_{11})}{2E} \right] \Delta P \quad (20)$$

where E – fiber Young's modulus, P_{11} and P_{12} are Pockells constants, which can be defined experimentally, n_{eff}^2 – effective refraction index and ν - Poisson's ratio. Sensor imaging objective lens will be illuminated by external illumination (or their light-emitting) scenery imaged on the image surface of the objective lens, forming a two-dimensional space of the optical sensor

(light intensity distribution), while being able to change the two-dimensional light intensity distribution of the optical sensor into a one-dimensional temporal electrical signal of such a class of sensors, we call the vision sensor [20]. Vision sensor variety, according to its decomposition of optical sensors in different ways, can be divided into three categories: electron beam scanning class, optical machine scanning class, and solid self-scanning class; in sensor mathematical model-data fusion, its optimization, in terms of application will be more efficient. Sensors are the material basis of information fusion, of which mathematical models and visual sensor sensors are the two types of fusion commonly used in information fusion, for certain optimization of existing sensors and increasing their efficiency. A mechanical wave with a frequency exceeding the frequency of an acoustic wave is known as ultrasound, which can propagate in liquids, gases, solids or living organisms. The relationship between ultrasound frequency, speed and wavelength is determined [21].

IV.COMPUTER MODEL

The main aim of computer model was to find an alternative to spectrum optical analyzer, which is an expensive instrument in optical area and to find alternative means of visualization of fiber Bragg grating's reflection spectrum in software to model MATLAB. In the MATLAB software selected for modeling, the coupling model theory and Transfer Matrix Method were formed for implementation into the MATLAB code. As well, in MATLAB software main FBG basic properties were used and selected to study external factors affect, such as deformation, stress and temperature, at FBG sensor's reflection spectrum.

In the work herein the authors developed MATLAB software with account of grating structure's parameters. Parameters under consideration are Bragg wavelength, effective index of grating refraction, factor of core refraction and grating structure's cladding, distance stroke between gratings, coupling coefficients of alternate and direct current and grating's length.

Figure 5 shows flow diagram of coupling modes theory and Transfer Matrix Method, recorded in Matlab codes.

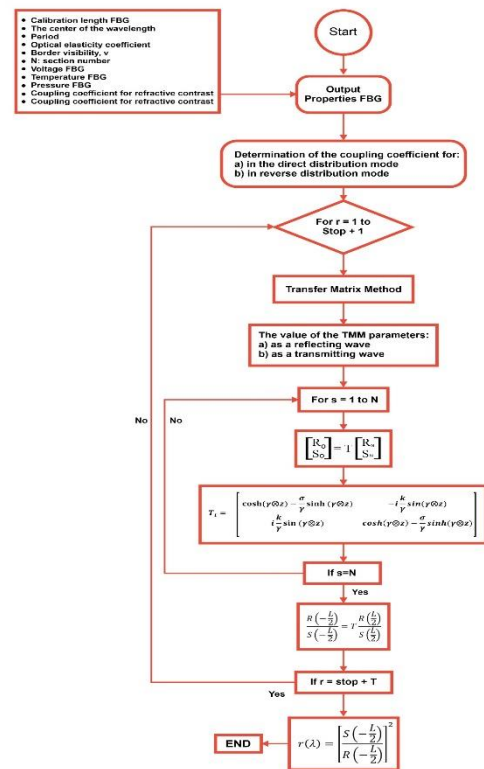


Figure 5. Flow diagram of coupling modes theory and Transfer Matrix Method

As for change of FBG grating wavelength, as far as grating length increases, bandwidth of reflected spectrum transmittance decreases, but spectrum's reflected capacity increases. It means, that the light, passed through grating sensor, reflected in each grating, and total reflected power increased. Results of modeling grating length change show spectrum decoupling due to absence of strain uniform distribution along FBG long grating to overcome the situation in the reflected spectrum.

V. MODELING SPECTRAL CHARACTERISTICS, APPLYING ORIGINAL MODELING APPLICATION

Understanding of characteristics and principal parameters of fiber Bragg gratings without necessity of their fabrication. But for that, there required modeling tools. Their usage might bring to minimize the risk of creating of abnormal grating, and also to correct the grating for target application earlier. Adequate choice of apodization function permits to optimize additionally grating characteristics with account of target application, for instance, as quality of optical filter or measurement sensor [17].

Own modeling tool, based on mathematical model, TMM, has been used for modeling transmittance spectrum change for various Bragg grating lengths. For that aim there was used Bragg grating with the wavelength of 1550 Nm with effective wavelength 1,447. Modeling outcomes are presented in Figure 1 below.

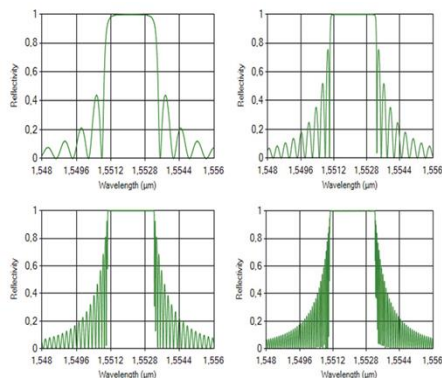


Figure 6. Characteristics of transmittance spectrum for different Bragg wavelengths (1 mm, 2 mm, 4 mm, 8 mm).

Figure 6 shows the characteristics of the transmittance spectrum for different Bragg wavelengths (1 mm, 2 mm, 4 mm, 8 mm). They have periodic modulation of the refractive index along the fiber axis, but they differ from VBR in that they have a certain angle of inclination between the lattice plane and the cross section of the fiber, which leads to a more complex interaction of modes. The main parameter of VBR is the wavelength of the Bragg resonance λ_B , which is also the central wavelength of the reflection and transmission spectra of the lattice. The introduction of a phase shift into the refractive index lattice leads to the appearance of a narrow transmission region inside the reflection band, the width of which can vary from several units to hundreds of picometers.

Legality of used tool has been confirmed with additional simulations for different Bragg wavelengths (1546 Nm, 1550 Nm). Results of observations were placed on sequential graphic charts, Figure 2.

Presented possibilities is only a part of accessible modeling parameters. It is possible to define apodization factor, used for Bragg gratings recording. However, that topic will be discussed in details in the following subsections of the article herein.

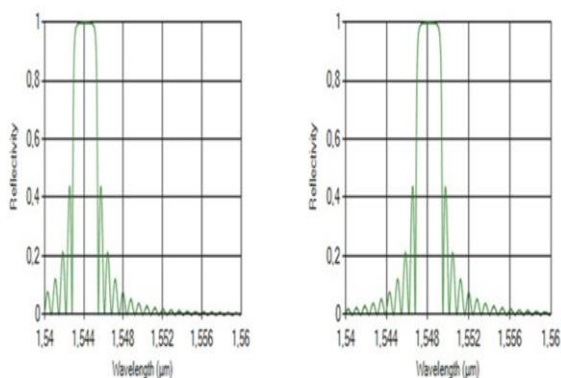


Figure 7. Transmittance spectrum for different Bragg wavelengths (1546 Nm, 1550 Nm).

Measurement of actual temperature sensors, based on fiber Bragg gratings was carried out, using climatic cell and Bragg grating, produced in strictly definite conditions. Figure 7 presents schematic system for fabrication of periodic fiber-optic structures, using phase mask. In such type of system the forceful irradiation beam in ultraviolet area is directed to elliptical lens,

focusing the light in one plane. Ray of compacted irradiation passes through phase mask, where interference structure is created, which provides forming of interference bands on the surface of being irradiated optical fiber.

Interference strings, which fall into separate fragments of optical fiber, bring to periodic change of refraction index in the core, which creates Bragg mirror. It should be noted, that the higher energy concentration in one band, created by interference picture of phase mask, the deeper modulation of refraction index, due to optical fiber irradiation in periodic structure. In case of fabricating Bragg gratings, using periodic phase mask, grating apodization is defined by distributing ray intensity, generated with excimer laser in lateral axle in reference to axle of fiber optic core, in which the grating was fabricated.

Novelty of the method herein is development of Bragg grating recording technique, using uniform phase mask. It consists of ultraviolet excimer laser, output beam of laser light, directed to the system of mobile diaphragms with regulated gap between them and located behind mobile diaphragms of uniform phase mask, behind which there is photosensitive multimode optical fiber with tilted Bragg grating.

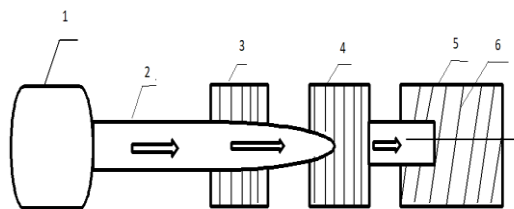


Figure 8. Scheme of installation for fabricating periodic structures in optical fibers, using phase mask method.

Technique of recording Bragg apodized gratings. Using uniform phase mask is characterized with the fact, that the width of the gap between mobile diaphragms 3 is in the range from 0,1 to 0,2 mm. Afterwards, ultraviolet excimer laser 1 radiates laser beam 2, appropriate for fabricating Bragg grating on mobile diaphragms 3 and after passing through mobile system the diaphragm 4 irradiates contracted laser beam on uniform phase mask 5, behind which is photosensitive multimode optical fiber with tilted Bragg grating 6, and a part of Bragg grating burns on photosensitive multimode optical fiber with tilted grating. Then the system of mobile diaphragms 3 moves along photosensitive multimode optical fiber with tilted Bragg grating 6 to the gap width, maintaining fixed gap width, afterwards the cycle is repeated till recording fixed Bragg grating. Graph in Figure 4 illustrates profile of cross section of laser beam, used for creating Bragg grating. Profile meter, used for measuring irradiation intensity along selected axle with with a pitch 1 μm. Assuming, that laser beam has 8 mm width, its profile has been specified in 8000 points of measurement. Based on the measured profile of the laser beam, the approximating

function was determined using the tools of the MatLab package. During the analysis, it was decided, that the adjustment of the Gaussian curve function is in the form:

$$f = a \cdot \exp\left(-\left(\frac{x-b}{c}\right)^2\right) \quad (21)$$

where: a = 0,9787; b = -551,7; c = 1960.

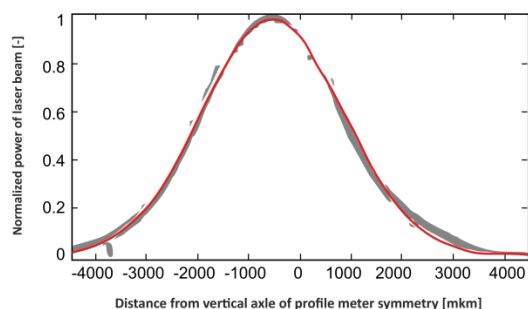


Figure 9. Profile of the laser beam with approximating Gaussian curve

Adjustment of the Gaussian curve with the above coefficients gave good statistical parameters (detection coefficient R2 = 0.9964 and root-mean-square error, RMSE, equal to 0.0204). Figure 5 shows the actual course of the laser beam profile and the approximation curve with parameters, expressed by the formula (21).

Modeling optical systems, using computer tools, based on mathematical models, can be very useful, but it is worth realizing, that machine language is not able to reproduce fully the physical optical system and all prevailing physical phenomena. In this part of the article, the simulated characteristics are compared with real reflection spectrum. It was found out, how the simulated object can differ from the actual system.

As part of the experiment, the Bragg grating was created in a system, similar to the one shown in Figure 9. A uniform phase mask with a constant period was used along its entire length. A laser with a beam profile, introducing apodization with a function, given by formula (12), was used to burn a periodic structure in the core of an optical fiber. In Figure 6, the reflected spectrum was measured using a spectrum analyzer with a resolution of 0.02 Nm.

In case of a mathematical model, similar lattice parameters were entered as input data for the modeling tool (the previously specified apodization function was taken into account). The results of this simulation are shown in Figure 9.

Comparison of the spectrum, shown in Figure 7 and the modeling characteristics, shown in Figure 8, clearly show the compatibility of the nature of Bragg grating with the model, used in the application. Both characteristics are consistent with the fact, that the use of an apodization with a profile, consistent with the Gaussian curve with appropriately chosen parameters leads to disappearance of side lobes common to homogeneous FBGs.

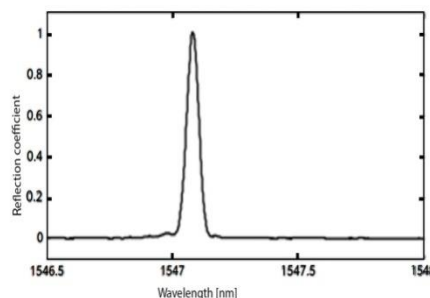


Figure 10. Reflection spectrum of real optical system

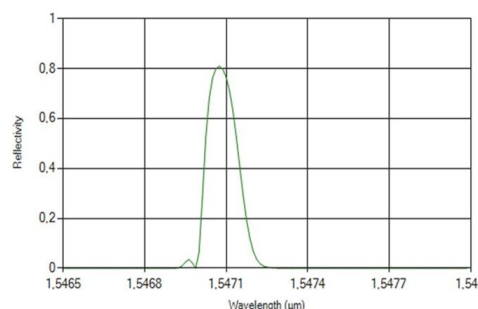


Figure 11. Simulated reflection spectrum of apodization spectrum in compliance with laser beam profile

Measurements to determine the temperature sensitivity of a sensor, based on FBG, are made on determining the Bragg wavelength, using spectral characteristics, measured over a range of different temperatures. The most commonly used method for determining the center wavelength is to find the extremum (minimum for the transmission spectrum or maximum for the reflection spectrum). Figure 8 shows a diagram of a measuring system, in which a climatic chamber was used to set the temperature. During the measurements, the relative humidity was maintained at constant 30%.

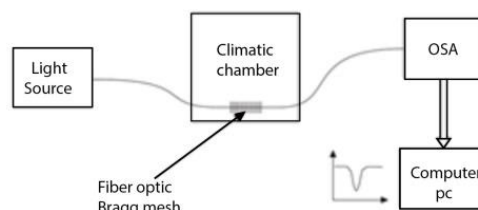


Figure 12. System diagram for determining processing characteristics

In Figure 12, the graph shows the processing characteristics of temperature sensor under test along a line with a linear regression, derived from the measurement points.

The linear correlation coefficient, obtained for the characteristic points in the measured temperature range is r = 0.9997 and the standard deviation is s = 0.473. These parameters show, that the nature of temperature changes depends on the change in the Bragg wavelength, and it is linear. The sensitivity of the system, understood as the amount of shift of the central wavelength up to 1 degree Celsius, can be expressed as the ratio of the difference in the Bragg wavelength at the measured temperatures to the difference between these temperatures:

$$\frac{\otimes \lambda_B}{\otimes T} = \frac{\lambda_{T1} - \lambda_{T2}}{T_1 - T_2} \quad (22)$$

Sensitivity S of tested sensor is defined in the following manner.

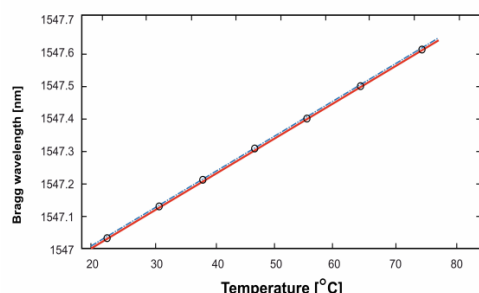


Figure 13. Parameters of temperature sensor processing

VI. CONCLUSION

This research work consisted in studying the mathematical model of FBG. The main goal of the study was to develop a computer model of a fiber Bragg grating sensor. Mathematical model parameters of FBG sensors such as calculated lambda, grating length, reflection, grating spacing and sigma change. The structure of the reflection spectra was built depending on each change in the simulation parameters. It can be seen, that changes in the grating pitch will change the amplitude of the Bragg wavelength. Changes to all other simulation parameters will affect the reflection spectrum of the FBG sensor. In fact, the strain, applied to the sensor, can be quantified by measuring the normalized amplitude of main lobe reflection capacity for the calculated Bragg wavelength. One way to eliminate unfavorable features of the spectrum is apodization, which usually includes modulation of the changes depth in the refractive index along the structure. Using a mathematical model, that takes into account the apodizing function and creating own simulation application, makes it possible to predict the effect of changes in the apodization parameters on the output spectrum. The examples show the effect of the selected simulation inputs on the shape of the output characteristic. In this study, it is used for the analysis of Gauss-apodized FBG sensors.

The quality of the model, used in the simulations was verified by comparing the parameters, measured for real Bragg grating, with the apodization, given by the laser beam profile to the resulting simulation outcome for introduced apodization function, corresponding to laser beam energy distribution. Both characteristics show obvious side-lobe suppression, adding a Gaussian character to the spectrum of the main peak.

Fiber Bragg grating, used as a temperature sensor, provides a linear characteristic of the measured quantity for shifting the center length of the grating wave. The experiment, performed for the fabricated grating, made it possible to determine its temperature sensitivity, which is 10.37 h/°C. The linear nature of the temperature processing for the Bragg wavelength deformation was confirmed, as evidenced by the noted characteristics of the statistical parameters.

ACKNOWLEDGMENTS

This work is supported by grant from the Ministry of Education and Science of the Republic of Kazakhstan within the framework of the Project № AP09259547 «Development of a system of distributed fibre-optic sensors based on fibre Bragg gratings for monitoring the state of building structures», Institute of Information and Computational Technologies CS MES RK. Experimental researches have been carried out in the laboratories of optoelectronics at the Electric engineering and computer sciences faculty of Lublin Technical University

REFERENCES

- [1] Kotyra, A., 2014. Optoelektroniczne systemy w zastosowaniach diagnostycznych i pomiarowych. Informatyka, Automatyka, Pomiary w Gospodarce i Ochronie Środowiska, 4(2), 9-10.
- [2] Pereira, G., McGugan M., Mikkelsen L.P., 2016. Method for independent strain and temperature measurement in polymeric tensile test specimen using embedded FBG sensors. Polymer Testing, 50,125-134.
- [3] Kashyap, R., 1999. Fiber Bragg Gratings. San Diego: Academic Press. Kenneth O., Meltz G., Fiber Bragg Grating Technology Fundamentals and Overview. Journal of Lightwave Technology, 15(8), 1263-1276.
- [4] Kenneth O., Meltz G., 1997. Fiber Bragg Grating Technology Fundamentals and Overview. Journal of Lightwave Technology, 15(8), 1263-1276.
- [5] Chen, Y., Chen, L., Liu, H., Wang, K., 2013. Research of FBG sensor signal wavelength demodulation based on improved wavelet transform. Optic, 124,4802-4804.
- [6] Negri, L., Nied, A., Kalinowski, H., Paterno, A., 2011. Benchmark for Peak Detection Algorithms in Fiber Bragg Grating Interrogation and a New Neural Network for its Performance Improvement. Sensors, 11, 3466-3482.
- [7] Ciężarczyk, S., Kisała, P., 2016. Inverse problem of determining periodic surface profile oscillation defects of steel materials with a fiber Bragg grating sensor. Appl. Opt. 55, 1412-1420
- [8] Harasim, D., Gulbakhar, Y., 2015. Improvement of FBG peak wavelength demodulation using digital signal processing algorithms. In: Proc. SPIE 9662, 966212, Photonics Applications in Astronomy, Communications, Industry and High-Energy Physics Experiments.

- [9] Kisała, P., Cięszczyk, S., 2015. Method of simultaneous measurement of two direction force and temperature using FBG sensor head. *Applied Optics* 54(10), 2677-2687.
- [10] Kisała, P., 2015. Method of simultaneous measurement of bending forces and temperature using Bragg gratings. In: *Proc. SPIE 9506, Optical Sensors 2015*.
- [11] Majumder, M., Gangopadhyay, T. K., Chakraborty, A. K., Dasgupta, K., Bhattacharya, D. K., 2008. Fiber Bragg gratings in structural health monitoring – present status and applications. *Sensors and Actuators*, 147,150- 164.
- [12] Harasim. D., Kisała, P., 2015. Układy przesłuchujące multipleksowane światłowodowe czujniki Bragga. *Informatyka, Automatyka, Pomiary w Gospodarce i Ochronie Środowiska*, 5(4), 77-84.
- [13] Abdulina, S. R., Vlasov, A. A., 2014. Suppression of side lobes in the fiber Bragg grating reflection spectrum. *Optoelectronics, Instrumentation and Data Processing*, 50(1), 75-86.
- [14] Demirdag, O., Yildirim, B., 2016. Comparing transfer matrix method and AN- FIS in free vibration analysis of Timoshenko columns with attachments. *Res. Eng. Struct. Mat.*, 2, 1-18.
- [15] Khalid, K. S., Zafrullah, M., Bilal, S. M., Mirza, M. A., 2012. Simulation and analysis of Gaussian apodized fiber Bragg grating strain sensor. *Journal of Optical Technology*, 7(10), 667-673.
- [16] Wójcik, W., Kisała, P., 2010. Metoda wyznaczania funkcji apodyzacji światłowodowych siatek Bragga na podstawie ich charakterystyk widmowych. *Przegląd Elektrotechniczny*, 86(10), 127-130.
- [17] Wójcik, W., Kisała, P., 2009. The application of inverse analysis in strain distribution recovery using the fiber Bragg grating sensors. *Metrology and Measurement Systems*, 16(4), 649-660.
- [18] Udoh, Solomon and Njuguma, James and Prabhu, Radhakrishna., 2014. Modeling and Simulation of Fiber Bragg Grating Characterization for Oil and Gas Sensing Applications. *Proceedings of the 2014 First International Conference on Systems Informatics, Modeling and Simulation*, 255260, IEEE Computer Society.
- [19] Santos, Jose Luis and Farahi, Faramarz., 2014. *Handbook of Optical Sensors*. CRC Press.
- [20] Fakhrazad, M and Goodarzi, F., 2021. A new multi-objective mathematical model for a Citrus supply chain network design: metaheuristic algorithms, *Journal of Optimization in Industrial Engineering*, 14(2),127–144.
- [21] Jaladi, A., Khithani, K., Pawar, P., Malvi, K and Sahoo, G., 2019. Environmental monitoring using wireless sensor networks (WSN) based on

IOT, *International Research Journal of Engineering and Technology*, 4(1),1371–1378.

- [22] El Afeni, A., Guettari, M., and Tajouri, T., 2021. Mathematical model of Boltzmann's sigmoidal equation applicable to the spreading of the coronavirus (Covid-19) waves, *Environmental Science and Pollution Research*, 28(30),40400–40408.

Contribution of Individual Authors to the Creation of a Scientific Article (Ghostwriting Policy)

Aliya Kalizhanova, Murat Kunelbayev, Ainur Kozbakova has organized and executed the experiments. Zhalau Aitkulov, Zhassulan Orazbekov carried out the simulation results, interpretation (discussion) and verification of results.

Creative Commons Attribution License 4.0 (Attribution 4.0 International, CC BY 4.0)

This article is published under the terms of the Creative Commons Attribution License 4.0

https://creativecommons.org/licenses/by/4.0/deed.en_US